Layer-by-Layer Self-assembly of a Polyelectrolyte Bearing Metal Ion Coordination and Electrostatic Functionality

Henning Krass, Georg Papastavrou, and Dirk G. Kurth*

Max Planck Institute of Colloids and Interfaces, D-14424 Potsdam, Germany

Received August 1, 2002. Revised Manuscript Received October 18, 2002

A novel polyelectrolyte (BiPE) bearing permanently charged quaternary ammonium groups as well as bipyridine ligands for metal ion recognition is presented that can be incorporated into ultrathin films either through electrostatic interactions or metal ion coordination. Conventional layer-by-layer assembly of BiPE with sodium poly(styrene sulfonate) (PSS) as an oppositely charged component results in multilayers. Layer growth is linear and the resulting films are smooth and homogeneous as indicated by X-ray reflectometry, ellipsometry, and atomic force microscopy (AFM). Reflection−absorption infrared spectroscopy suggests that the counterions are exchanged during layer assembly. The BiPE/PSS multilayers can bind transition metal ions including Fe(II), Ni(II), and Zn(II). Metal ion release from the layer is induced by ethylenediaminetetraacetic acid (EDTA), a strong complexing agent. Formation of 2-D arrays of metallo-units is achieved by microcontact stamping transition metal salts onto the BiPE/PSS interface. Also, multilayers of BiPE are readily assembled through metal ion coordination. The importance of metal ion coordination for multilayer formation is demonstrated by force−distance curves measured with AFM. Due to the reversible nature of metal ion coordination, exposure of these multilayers to EDTA causes instant disassembly of the layer, a property needed to implement stimulus-triggered release functions.

Introduction

Recently, the subsequent deposition of oppositely charged polyelectrolytes has become a widespread procedure to fabricate well-defined thin films. The interest in the so-called *el*ectrostatic layer-by-layer *s*elf-*a*ssembly (ELSA) method rests on the simplicity of layer formation, the excellent thickness control, and its broad applicability. The popularity of this approach can be seen in the ability to tailor the structural and functional properties of thin films.[1] When multilayer formation is started from patterned surfaces, it can be directed to specific regions on the substrate.[2,3] While earlier work focused on coating planar substrates, recent developments also include particle coatings. In the case of strong polyelectrolytes, electrostatic interactions are commonly accepted as primary forces providing multiple-point adhesion within adjacent layers.[4] Other intermolecular forces have also been implemented including hydrogen bonding,[5] charge transfer,[6] and acid-based interactions.[7] In particular, weak polyelectrolytes offer opportunities to render the structural, morphological, and functional properties solely by pH.[8]

For these reasons, it is safe to predict that the realization of thin film devices will be the future trend both in fundamental and applied research.[9] To encode new properties and to manage device performance, it will be of critical importance to control position and orientation of the functional components in final device architecture. While further progress toward these goals calls for substantial research efforts, we can count on fascinating rewards circumventing some of the intrinsic problems of conventional device fabrication: parallel fabrication, (molecular) dimension control, and thermodynamically driven self-repair. As charge is the chief requirement for successful ELSA processing, an almost unlimited range of functional components lies ahead to be implemented into layered architectures: examples include nanoparticles for light-emitting diodes,[10] electroluminescent heterostructures,[11] enzyme electrodes for sensing,[12] composite membranes for separation,[13]

* To whom correspondence should be addressed. Tel: 0331-567 9211. Fax: 0331-567 9202. E-mail: kurth@mpikg-golm.mpg.de.

(1) Dubas, S. T.; Schlenoff, J. B. *Macromolecules* **1999**, *32*, 8153−8160.
(2) Hammond, P. T.; Whitesides, G. M. *Macromolecules* **1995**, *28*, 7569−7571.
(3) Decher, G.; Lehr, B.; Lowack, Y.; Lvov, J.; Schmitt, J. *Biosens. Bioelectron.* **1994**, *9*, 677−684.
(4) Netz, R. R.; Joanny, J. F. *Macromolecules* **1999**, *32*, 9013−9025.
(5) Sukhishvili, S. A.; Granick S. *Macromolecules* **2002**, *35*, 301−310.
(6) Shimazaki, Y.; Ito, S.; Tsutsumi, N. *Langmuir* **2000**, *16*, 9478−9482.
(7) Hammond, P. T. *Curr. Opin. Colloid Interface Sci.* **1999**, *4*, 430−442.
(8) Shiratori, S.; Rubner, M. F. *Macromolecules* **2000**, *33*, 4213−4219.
(9) Swalen, J. D.; Allara, D. L.; Angrade, J. D.; Chandross, E. A.; Garoff, S.; Israelachvili, J.; McCarthy, T. J.; Murray, R.; Pease, R. F.; Rabolt, J. F.; Wynne, K. J.; Yu, H. *Langmuir* **1987**, *3*, 932−950.
(10) Gao, M. Y.; Richter, B.; Kirstein, S. *Adv. Mater.* **1997**, *9*, 802−805.
(11) Onitsuka, O.; Fou, A. C.; Ferreira, M.; Hsieh, B. R.; Rubner, M. F. *J. Appl. Phys.* **1996**, *80*, 4067−4071.
(12) Anicet, N.; Bourdillon, C.; Moiroux, J.; Savenant, J. M. *J. Phys. Chem. B* **1998**, *102*, 9844−9849.

10.1021/cm020808d CCC: $25.00
Published on Web 12/03/2002

polyoxometalate clusters for electrochromic devices[14] and as nanoreactors,[15] to name just a few examples.

Metal ion−ligand interactions are a widespread recognition motive in supramolecular chemistry. The metal ion collects and orients the organic ligands in space. Metal ions have properties that are of special interest for functional devices.[16] They provide a set of coordination geometries, a range of binding strengths, and ligand exchange kinetics, which are needed for reversible and switchable interaction sites. The ability to interact with photons and electrons alike makes metal ion coordination compounds or metallo-units particularly suitable as functional components in devices and materials. Strong absorption and luminescence together with high quantum yields and suitable excited-state lifetimes make them promising candidates for components in photonic devices. In addition, metal ions possess interesting magneto-optical properties that are relevant for the construction of advanced materials.[17] Using metal ion−ligand interactions in film fabrication, therefore, offers interesting perspectives including reversible interaction sites for controlled assembly and release as well as sensing. Characteristic absorption bands and fluorescence as well as a rich electrochemistry can be utilized to investigate film formation, structure, and properties. The modular nature of metal ion coordination provides means for tailoring structure and function of the films from molecular to macroscopic levels.[18]

Despite the promising assets of metallo-units little work has been done to incorporate the value-adding properties of these systems into thin films.[19] Generally, discrete metal ion complexes do not form regular ELSA multilayers because they possess too few charges to irreversibly adsorb on charged interfaces.[20] As we have shown recently, introducing secondary interactions through $\pi-\pi$ stacking of aromatic moieties in the metal ion complex stabilizes the resulting assembly at an interface, resulting in irreversible adsorption.[21] Another method toward this goal relies on metallo-supramolecular coordination polyelectrolytes (MEPEs).[22] Due to the high charge of these macromolecular assemblies, they adsorb irreversibly on charged interfaces,[23] including nanoparticles.[24] The resulting films are robust and the electrochemical properties of the central metal ions are fully preserved in the multilayer.[25]

In the following presentation, some of the perspectives and potential features of metal ion coordination as a binding motive in thin films are investigated. This first account is meant as a proof of principle and employs for this purpose a novel polyelectrolyte capable of metal ion binding through bipyridine receptors. Through the conventional ELSA protocol multilayers are fabricated capable of reversibly binding transition metal ions. Imprinting transition metal ions onto these layers leads to mesoscopically structured 2-D arrays of metallo-units. In addition, metal ion coordination is explored as a binding motive to assemble multilayers. The adhesive force arising from metal ion coordination between adjacent BiPE layers is demonstrated by performing adhesion experiments by means of AFM. The reversible metal ion−ligand interaction provides a means to deliberately assemble and disassemble this type of multilayer.[26]

Experimental Section

Synthesis of BiPE. The synthesis of BiPE was achieved starting from 4,4′-dimethyl-2,2′-bipyridine. Oxidation to the diacid with CrO_3 in sulfuric acid (yield 75%),[27] conversion to the dimethylester in methanol/sulfuric acid (yield 81%)[3], reduction by $NaBH_4$ to the di-alcohol (yield 88%)[28] followed by treatment with HBr[29] gave 4,4′-dibromo-2,2′-bipyridine (yield 50%). The dibromobipyridine was treated in acetonitrile with 1,3-*N*,*N*,*N*′,*N*′-tetramethyl-1,3-diaminopropane.[30] The BiPE precipitated as white solid and was isolated by filtration (yield 54%). ^{1}H NMR ($CDCl_3$, room temperature): δ 8.71 (d, $J = 4.8$, 2H), 8.26 (s, 2H), 7.64 (d, $J = 4.8$, 2H), 4.6 (br, 4H), 3.51(br, 4H), 3.14 (br, 12H), 2.54 (br, 2H). Elemental analysis. Calculated for $[C_{19}H_{28}Br_2N_4(H_2O)_3]_{17}$, $M = 8947$ g/mol: C, 43.4; H, 6.5; N, 10.6. Found: C, 43.1; H, 6.2; N, 10.5. UV/vis (H_2O): $\pi-\pi^*$ bands at 237 and 289 nm. IR (KBr): 3008, 2962, 1597, 1558, 1482, 1432, 1387, 1315, 1221, 1112, 1052, 993, 836, 760 cm^{-1}. Investigation by ^{1}H NMR end group analysis and analytical ultracentrifugation showed that BiPE consists of 17 ± 3 repeat units. The Fe−BiPE complex was isolated by adding an aqueous solution containing $(NH_4)_2Fe(SO_4)_2$ to an aqueous solution of BiPE, which resulted instantly in a deep red coloration ($\lambda_{max} = 538$ nm, $\epsilon = 8800$ M^{-1} cm^{-1}).

(13) Kraseman, L.; Tieke, B. *Langmuir* **2000**, *16*, 287−290.
(14) Liu, S.; Kurth, D. G.; Möhwald, H. *Adv. Mater.* **2002**, *14*, 225−228.
(15) Kurth, D. G.; Volkmer, D.; Ruttorf, M.; Richter, B.; Müller, A. *Chem. Mater.* **2000**, *12*, 2829−2831.
(16) (a) Holliday, B. J.; Mirkin, C. *Angew. Chem., Int. Ed.* **2001**, *40*, 2022−2043. (b) Kurth, D. G. *Ann. N. Y. Acad. Sci.* **2002**, *960*, 29−39.
(17) (a) Decurtins, S.; Gütlich, P.; Kohler, C. P.; Spiering, H.; Hauser, A. *Chem. Phys. Lett.* **1984**, *105*, 1−4. (b) Decurtins, S.; Gütlich, P.; Hasselbach, K. M.; Hauser, A.; Spiering, H. *Inorg. Chem.* **1985**, *24*, 2174−2178. (c) Renz, F.; Osio, H.; Ksenofontov, V.; Waldeck, M.; Spiering, H.; Gütlich, P. *Angew. Chem., Int. Ed.* **2000**, *39*, 3699−3700. (d) Gu, Z. Z.; Sato, O.; Iyoda, T.; Hashimoto, K.; Fujishima, A. *J. Phys. Chem.* **1996**, *100*, 18289−18291. (e) Sato, O.; Iyota, A.; Fujishima, A.; Hashimoto, K. *Science* **1996**, *272*, 704−705. (f) Attia, A. S.; Jung, O. S.; Pierpont, C. G. *Inorg. Chim. Acta* **1994**, *226*, 91−98. (g) Boillot, M.-L.; Roux, C.; Audiere, J.-P.; Dausse, A.; Zarembowitch, J. *Inorg. Chem.* **1996**, *35*, 3975−3980.
(18) Kurth, D. G.; Lehmann, P.; Schütte, M. *Proc. Natl. Acad. Sci. U.S.A.* **2000**, *97*, 5704−5707.
(19) For examples of thin films constructed with metal coordination interactions, see: (a) Mallouk, T. E.; Gavin J. A. *Acc. Chem. Res.* **1998**, *31*, 209−217. (b) Maskus, M.; Abruna, H. D. *Langmuir* **1996**, *12*, 4455−4462. (c) Liang, Y.; Schmehl, R. *Chem. Commun.* **1995**, 1007−1008. (d) Hatzor, A.; van der Boom-Moav, T.; Yochelis, S.; Vaskevich, A.; Shanzer, A.; Rubinstein, I. *Langmuir* **2000**, *16*, 4420−4423.
(20) Unpublished results. If the bulk concentrations are identical and if nonelectrostatic interactions can be neglected, the surface coverage of a polyion with charge z exceeds that of a monovalent ion by e^z, that is, an ion with four charges adheres 55 times more strongly than a monovalent ion (Israelachvili, J. *Intermolecular &Surface Forces*, 2nd ed.; Academic Press: New York, 1995).
(21) Krass, H.; Plummer, E. A.; Haider, J. M.; Barker, P. R.; Alcock, N. W.; Pikramenou, Z.; Hannon, M. J.; Kurth, D. G. *Angew. Chem., Int. Ed.* **2001**, *40*, 3862−3865.
(22) Schütte, M.; Kurth, D. G.; Linford, M. R.; Cölfen, H.; Möhwald, H. *Angew. Chem., Int. Ed.* **1998**, *37*, 2891−2893.
(23) Kurth, D. G.; Osterhout, R. E. *Langmuir* **1999**, *15*, 4842−4846.
(24) (a) Kurth, D. G.; Caruso, F.; Schüler, C. *Chem. Commun.* **1999**, *16*, 1579−1580. (b) Caruso, F.; Schüler, C.; Kurth, D. G. *Chem. Mater.* **1999**, *11*, 3394−3399.
(25) Kurth, D. G.; Schütte, M.; Wen, J. *Colloids Surf., A* **2002**, *198*, 633−643.
(26) Previously, hydrogen bonding was used in reversible interaction to assemble and disassemble thin films (Sukhishvili, S. A.; Granick, S. *J. Am. Chem. Soc.* **2000**, *122*, 9550−9551. Dubas, S. T.; Schlenoff, J. B. *Macromolecules* **2001**, *34*, 3736−3740.)
(27) Garelli, N.; Vierling, P. *J. Org. Chem.* **1992**, *57*, 3046−3051.
(28) Ciana, L. D.; Dressick, W. J.; Zelewsky, A. *J. Heterocycl. Chem.* **1990**, *27*, 163−165.
(29) Berg, K. E.; Tran, A.; Raymond, M. K.; Abrahamsson, M.; Wolny, J.; Redon, S.; Andersson, M.; Sun, L.; Styring, S.; Hammarstroem, L.; Toftlund, H.; Akermark, B. *Eur. J. Inorg. Chem.* **2001**, *4*, 1019−1029.
(30) Factor, A.; Heinsohn, G. E. *Polym. Lett.* **1971**, *9*, 289−295.

If more than 0.88 equiv of $(NH_4)_2Fe(SO_4)_2$ was added, a red solid precipitates.

Chemicals. All chemicals (Aldrich) were used as received. The following aqueous solutions were used: polyethylenimine (PEI, 10^{-2} M), sodium poly(styrene sulfonate) (PSS, 10^{-2} M), BiPE (10^{-3} M), and $(NH_4)_2Fe(SO_4)_2$ (4×10^{-3} M). If not stated otherwise, solutions contained 1 M NaCl. The concentrations of the polyelectrolytes are based on the molecular weight of the monomer unit.

Substrates. The substrates were cleaned by immersion in a solution containing 1 part NH_4OH (29 wt % aqueous solution), 1 part H_2O_2 (30 wt % aqueous solution), and 5 parts pure water at 70 °C for 20 min, followed by rinsing in water. Quartz glass (Hellma Optik, Jena, Germany) substrates were used for UV/vis spectroscopy. For XRR measurements polished silicon wafers (Wacker Chemie GmbH, Germany) were employed. Evaporated gold on glass slides, modified with a layer of mercaptopropionic acid, were used for FTIR measurements.

Instrumentation. UV/vis spectra were recorded with a Varian Cary 50 spectrometer. Reflection−absorption infrared (RAIR) spectra were recorded with a Bruker Equinox 55/S spectrometer operating in the reflection mode with a modified reflection accessory from Harrick (angle of incidence 84°). Static-polarization-modulated RAIR spectra were recorded by successively accumulating 50 scans with the polarized set at 0° or 90°.[31] A total of 500 scans were recorded. X-ray reflectance (XRR) measurements were performed on a unit from STOE&CIE (Darmstadt, Germany). $U = 40$ kV, $I = 50$ mA, $\lambda = 1.54$ Å (Cu Kα). The reflectance curves were fitted with a box model described elsewhere.[32] Ellipsometric measurements were performed with null-ellipsometry using a Multiskop (Optrel Germany, 2-mW HeNe Laser, $\lambda = 632.8$ nm, angle of incidence 70°). Films were deposited onto silicon wafers for these measurements. The real part of the refractive index (1.585) was determined from thick films.

Preparation of ELSA Films with Electrostatic Interactions. The cleaned substrates were immersed in a PEI solution for 20 min, rinsed with water, and dried with a gentle stream of nitrogen. Multilayers were prepared by alternatingly dipping the substrate in PSS and BiPE solutions. After each deposition step, the wafer was rinsed with water and dried with a gentle stream of nitrogen.

Microcontact Patterning. Microcontact stamping was performed by dabbing a polysiloxane stamp with a tissue paper drenched in $(NH_4)_2Fe(SO_4)_2$ solution. The stamp was applied to the coated quartz glass for 1 min; the wafer was rinsed with water and dried.

Preparation of Films with Coordinative Interactions. The cleaned substrate is first coated with a layer of PEI, PSS, and BiPE. Different protocols were applied for multilayer formation. A: The substrate was immersed in aqueous solutions of $(NH_4)_2Fe(SO_4)_2$ for 10 min. Excess fluid was removed either with a stream of nitrogen or by placement of one side of the substrate on a paper tissue. This step minimizes contamination of the BiPE solution. Then the substrate was immersed in the BiPE solution for 20 min, followed by rinsing with water and drying. B: The substrate was rinsed in water after each Fe(II) deposition. C: The substrate was rinsed in water after each deposition step.

AFM Measurements. The Si_3N_3 cantilevers (DI Instruments) were modified by attaching borosilicate particles (diameter ~10−15 μm, Planno, Germany) with EPOTEK 353N glue to the cantilevers apex and curing the glue at 45 °C for 4 h. The cantilevers' force constants were determined prior to the attachment of the particles by the method of Hutter and Bechöfer.[33] Polyelectrolyte deposition on the particles probes was carried out according to the above-mentioned procedure using a homemade Teflon holder for the cantilevers during the deposition process. Prior to the poylelectrolyte deposition process, the probes were cleaned by air plasma (Harrick Plasma Cleaner). The force measurements were carried out with a D3000 (Digital Instruments) equipped with an open fluid cell configuration. Measurements in one series were always performed with the same probe, exchanging only the substrate or the electrolyte solutions in which the measurements were carried out. Detection of adhesion events in the force−distance curves was performed with a slightly modified algorithm according to Gergely et al.[34] Employing an identical set of parameters for all data enables a direct comparison.

Scheme 1. Structure of the Bifunctional Polyelectrolyte (BiPE) Bearing Bipyridine Metal Ion Receptors and Positively Charged Ammonium Groups[a]

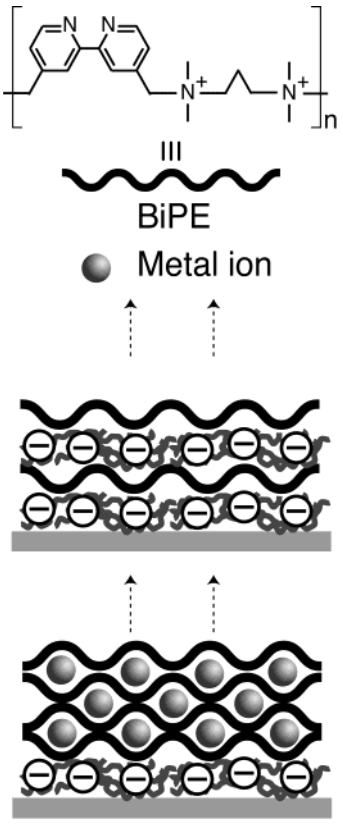

[a] The polyelectrolyte can be assembled through electrostatic interactions with negatively charged polymers, such as PSS (top). These layers can reversibly accept and release transition metal ions. In addition, layers can be fabricated directly through metal ion coordination (bottom). With a competing complexing agent the layers are readily disassembled. (The illustration is a simplification and shall not imply a layered architecture.)

Results and Discussion

First, we will discuss ELSA of BiPE with PSS and metal ion binding of the resulting BiPE/PSS multilayers, followed by patterning these layers by microcontact printing. Then, we describe a procedure to assemble multilayers through metal ion coordination and investigate the influence of metal ion−ligand interactions on the adhesion in these multilayers as determined by force−distance curves measured with AFM (Scheme 1).

Multilayers through Electrostatic Interactions. The quaternary ammonium groups in BiPE provide intrinsic and permanent charges that open a route for

(31) Kurth, D. G. *Langmuir* **1998**, *14*, 6987−6991.
(32) Asmussen, A.; Riegler, H. *J. Chem Phys.* **1996**, *104*, 8159−8164.
(33) Hutter, J. L.; John Bechhoefer. *Rev. Sci. Instrum.* **1993**, *64*, 1868−1873.
(34) Gergely, C.; Senger, B.; Voegel, J. C.; Horber, J. K.; Schaaf, P.; Hemmerle, J. *Ultramicroscopy* **2000**, *87*, 67−78.

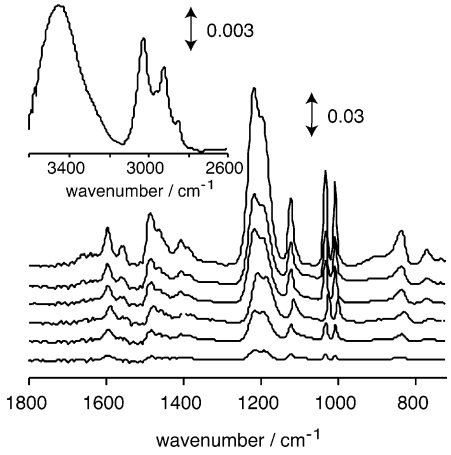

Figure 1. Reflectance absorbance IR spectra of PEI(PSS/BiPE)$_n$ multilayers ($n = 1-5, 10$) on gold substrates. The insert shows the IR absorbance in the CH stretching region ($n = 10$).

fabricating ELSA multilayers with oppositely charged polyelectrolytes, such as PSS. In addition, the quaternary ammonium groups facilitate solubility of BiPE in aqueous solution. To begin the ELSA procedure, the cleaned substrate is coated with a layer of PEI, which acts as an adhesion promoter for the subsequently deposited PSS layer. Multilayers are deposited onto the PEI/PSS cushion by alternating immersion in solutions containing BiPE and PSS and intermittent washing steps. Initial experiments are carried out in 1 M NaCl solutions.

Layer growth is investigated by UV/vis and reflectance absorbance IR (RAIR) spectroscopy. The absorbance in both UV/vis and RAIR spectroscopy increases linearly with the number of layers, indicating regular and linear multilayer growth. This result implies that equal amounts of polyelectrolyte are adsorbed at the interface in each step. Also, the band positions and contours do not change during layer growth. However, we note that the bandwidth in the RAIR spectra of a multilayer is reduced by up to one-half compared to transmission spectra of the neat components (not shown). Inhomogeneous band-broadening mechanisms are caused by perturbations associated with molecular interactions.[35] Apparently, such interactions are diminished in the multilayer, possibly because of the compound composition, which moderates direct interactions.

Representative RAIR spectra of PEI(PSS/BiPE)$_n$ ($n = 1, 2, 3, 4, 5, 10$) multilayers are shown in Figure 1. From the position of the sulfonate modes in the RAIR spectra we can draw conclusions about the nature of the counterion.[36] In the first PSS layer deposited on PEI, the sulfonate band splitting is 43 cm^{-1}, which is similar to neat Na−PSS. Most likely, there is no complete counterion exchange in the initial PSS layer. In the (BiPE/PSS)$_n$ multilayers the asymmetric stretching modes of the sulfonate group are located at 1197 and 1218 cm^{-1}. The smaller splitting of 21 cm^{-1} indicates that the Na ions are replaced by less polarizing ions such as the bulky tetra-alkylammonium groups. The symmetric stretching mode of the sulfonate group at 1034 cm^{-1} is hardly affected by the counterion. Also, we can rule out the presence of sulfonic acid groups; the characteristic modes at 1350, 1172, and 1097 cm^{-1} are clearly absent. A broad band at 3400 cm^{-1} indicates that the multilayers are hydrated (insert Figure 1).

From the UV/vis spectra the surface coverage can be calculated. If reflection losses are negligible, the surface coverage per layer is given by $\Gamma = [A_\lambda/(l \cdot e_\lambda)]$ (A_λ is the absorbance and e_λ is the molar extinction coefficient at wavelength λ; λ is the total number of layers). Using the characteristic absorbance of BiPE at 290 nm (e = 12770 M^{-1} cm^{-1}), the surface coverage amounts to 1.7 $\times$ 10^{-6} mmol of bipyridine units per cm^2, which corresponds to an area of 10 Å^2 per chromophore. Assuming a length of approximately 10 Å, a height of approximately 5 Å, and a width of approximately 3.5 Å, the average surface area of a bipyridine unit varies from approximately 17 to 50 Å^2 depending on the orientation. In the case of an isotropic distribution within the film, the average surface area amounts to approximately 34 Å^2. Apparently, BiPE adsorbs in a coiled conformation at the interface such that up to three bipyridine chromophores constitute a single layer. A coiled conformation of the polyelectrolyte is expected in aqueous solution at high ionic strength.[37] The coverage can be adjusted by the salt concentration in the adsorbate solutions as commonly observed for ELSA multilayers. Smaller coverages are observed if no salt is added to the BiPE solution (not shown).[38]

To elucidate the internal structure as well as the interfacial roughness, the multilayers were subjected to X-ray reflectivity (XRR) measurements. For example, a PEI(PSS/BiPE)$_3$PSS film shows as much as seven Kiessig fringes in the reflectance curve, which demonstrates that the multilayer is homogeneous in thickness and composition.[39] The reflectance curve is fitted by a standard box model to retrieve the thickness, electron density, and roughness. A detailed analysis reveals a film thickness of 205 Å and a roughness of approximately 10 Å. The SiO thickness is 6 Å. The corresponding electron densities, expressed as the parameter δ, are 7.44 $\times$ 10^{-6} for the silicon substrate, 7.33 $\times$ 10^{-6} for the Si−O layer, and 3.2 $\times$ 10^{-6} for the multilayer. These data are in agreement with values expected for these materials.[40] Similarly, the multilayer PEI(PSS/BiPE)$_2$PSS has a thickness of 134 Å. The average thickness per PSS/BiPE layer pair, therefore, amounts to 56 Å. Independent measurements of the thickness by optical ellipsometry confirm these results. The layer thickness is in agreement with the surface coverage determined by UV/vis spectroscopy.

Metal Ion Coordination and Exchange in PSS/BiPE Multilayers. The (PSS/BiPE)$_n$ multilayers have the intrinsic propensity to coordinate transition metal cations due to the bipyridine groups. With many transition metal ions bipyridine forms octahedral tris−bipyridine complexes with the general formula M(bipy)$_3$. With Fe(II) complex formation is particularly strong[41] and gives rise to characteristic and strong metal-to-ligand-

(35) Kurth, D. G.; Schütte, M. *Macromol. Symp.* **2001**, *164*, 167−179.
(36) Zundel, G. *Hydration and Intermolecular Interactions*; Academic Press: New York, 1969.
(37) Ladam, G.; Schaad, P.; Voegel, J. C.; Schaaf, P.; Decher, G.; Cuisinier, F. *Langmuir* **2000**, *16*, 1249−1255.
(38) Decher, G.; Schmitt, J. *Prog. Colloid Polym. Sci.* **1992**, *89*, 160−164.
(39) Kiessig, H. *Ann. Phys.* **1931**, *10*, 769−788.
(40) Russel, T. P. *Mater. Sci. Rep.* **1990**, *5*, 171−271.

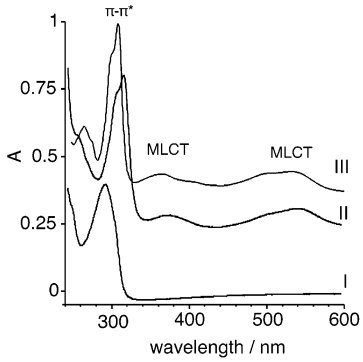

Figure 2. UV/vis spectra of a PEI(PSS/BiPE)$_8$ multilayer before (I) and after (II) immersion in Fe(II) solution and of $(NH_4)_2Fe(bipy)_3(SO_4)_2$ in aqueous solution (III).

charge-transfer (MLCT) bands in the UV/vis spectrum.[42]

Figure 2 shows the UV/vis absorption spectra of the $(NH_4)_2Fe(bipy)_3(SO_4)_2$ complex and of a PEI(PSS/BiPE)$_8$ multilayer before and after metal ion insertion. The neat $Fe(bipy)_3^{2+}$ complex shows MLCT bands at around 350 and 530 nm (spectrum III). Initially, the PEI(PSS/BiPE)$_8$ multilayer shows the characteristic bipyridine intraligand transitions at 247 and 290 nm (spectrum I). After metal ion coordination, the absorption band at 290 nm shifts to 310 nm, indicative for metal ion coordination. Furthermore, new bands at 371 and 540 nm appear, which are assigned to MLCT bands (spectrum II). The similarity of the spectra of (PSS/Fe(II)−BiPE)$_8$ and $Fe(bipy)_3^{2+}$ in solution in terms of band positions and relative intensities confirms formation of the tris−bipyridine Fe(II) complex in the multilayer.[43] The slight shift of the $\pi-\pi^*$ transition in spectra II and III is attributed to changes in the local environment.

The number of Fe(II) ions incorporated in the multilayer can be estimated from the absorption spectrum. Using the extinction coefficient of $(NH_4)_2Fe(bipy)_3(SO_4)_2$ determined in water (ϵ(530 nm) = 8800 M^{-1} cm^{-1}), we calculate a surface coverage of 6.2×10^{-7} mmol/cm^2. On the basis of the surface coverage of bipyridine in the multilayer (1.7×10^{-6} mmol/cm^2) (vide supra), we anticipate a coverage of 5.7×10^{-7} mmol/cm^2 in the case of $Fe(bipy)_3^{2+}$ formation. Within the experimental error, we can conclude that most if not all bipyridine groups in the multilayer engage in metal ion coordination. This result is interesting because it implies that the bipyridines in the multilayer possess sufficient mobility to conform to the steric demands required for octahedral coordination.[44]

To demonstrate the reversibility of metal ion coordination within the multilayer, the Fe(II)-containing multilayer is exposed to ethylenediaminetetraacetic acid (EDTA). In basic solution, EDTA has a strong propensity to coordinate Fe(II) (pK = 14 at pH 11).[45] In solution EDTA instantly decomplexes $Fe(bipy)_3^{2+}$ and forms a complex with Fe(II). Removal of the Fe(II) ions from the multilayer is readily confirmed by UV/vis spectroscopy,

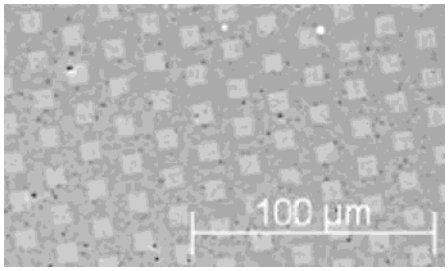

Figure 3. Phase-contrast microscopy image of a patterned PEI(PSS/BiPE)$_{10}$ surface. Lateral patterning with Fe(II) ions is achieved by microcontact stamping of the metal salt. The continuous dark area represents the imprinted (PSS/Fe(II)−BiPE) region. (The contrast was enhanced using digital editing.)

in particular by the disappearance of the MLCT bands (not shown). The coordination and release of metal ions is a reversible, even though slow, process. We note a residual absorbance of the MLCT band after immersing the multilayer in EDTA solution for 21 h (50 °C), which implies that not all Fe(II) ions are extracted. If the immersion time is extended to 4 days, the removal of Fe(II) is close to quantitative. Possibly, the reduced mobility of the polyelectrolyte segments in the multilayer slows down the exchange process.[46] Metal ion release requires simultaneous release of three bipyridine receptors within the polyelectrolyte matrix, followed by coordination to EDTA. On the other side, complexation of the multilayer by Fe(II) is completed in 45 min, when the MLCT band reaches a constant absorbance. Apparently, diffusion of Fe(II) into the multilayer and subsequent coordination by the (prearranged) bipyridine receptors is faster than the reverse process. Due to the versatile coordination chemistry of bipyridine, incorporation of other metal ions, such as Ni(II) or Zn(II), in these layers gives similar results. In the case of Zn(II), metal ion coordination is accompanied by multilayer fluorescence (not shown). The similarity of the fluorescence spectra of (PSS/Zn(II)−BiPE) and Zn(bipy)$^{2+}$ in solution confirms formation of the tris−bipyridine Zn(II) complex.

Lateral Patterning with Metal Ion Coordination. The immobilization of metal ion receptors at the interface offers the possibility to confine metal ions to predefined areas. Lateral patterning of the surface is achieved by microcontact stamping the transition metal salt on the (PSS/BiPE) multilayer followed by rinsing with water.

Figure 3 shows a representative microscopy image of a quartz slide coated with 10 BiPE/PSS layers after microcontact stamping of $(NH_4)_2Fe(SO_4)_2$. The darker area in the image corresponds to regions where salt is imprinted. UV/vis spectroscopy of the sample confirms metal ion coordination and complex formation. We, therefore, conclude that microcontact stamping of the transition metal salt results in spatial confinement of metallo-units. The fact that the metallo-pattern is preserved after rinsing demonstrates the high fidelity of metal ion−ligand interactions and the thereby resulting spatial confinement of the metal ions in the multilayer.

Multilayer Formation with Coordinative Interactions. In a second approach, we explore the metal

(41) McWhinnie, W. R.; Miller, J. D. *Adv. Inorg. Radiochem.* **1969**, *12*, 135−215.
(42) Constable, E. C. *Adv. Inorg. Chem.* **1989**, *34*, 1−63.
(43) Bryant, G. M.; Fergusson, J. E.; Powell, H. K. J. *Aust. J. Chem.* **1971**, *24*, 257−273.
(44) Caruso, F.; Lichtenfels, H.; Donath, E.; Möhwald *Macromolecules* **1999**, *32*, 2317−2328.
(45) Jander Blasius, *Einführung in das anorganisch-chemische Praktikum*, 12. Auflage, S. Hirzel Verlag: Stuttgart, 1987; p 323.
(46) Lowack, K.; Helm, C. A. *Macromolecules* **1995**, *28*, 2912−2921.

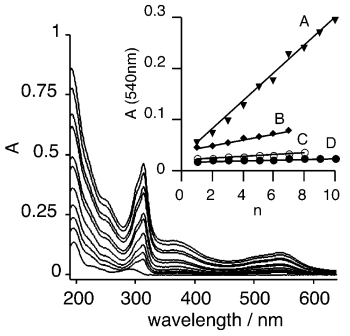

Figure 4. UV/vis spectra of BiPE on a quartz substrate deposited by metal ion coordination. The bottom trace shows the $\pi-\pi^*$ transition of uncoordinated bipyridine at 290 nm. Interlayer linkage by metal ion coordination shifts the band to 314 nm. Metal ion coordination is also confirmed by the characteristic MLCT transition at 542 nm. The insert shows the increase of absorbance at 541 nm as a function of the number of layers for different adsorption procedures: A: rinsing in water after each BiPE adsorption, B: rinsing in water after each Fe(II) ion deposition, C: rinsing in water after each deposition step, D: attempt of multilayer formation under omission of Fe(II) ion deposition.

ion−ligand interaction to form coordination bonds between adjacent BiPE layers. First, we generate a PEI/PSS/BiPE cushion, onto which subsequent BiPE layers are deposited through metal ion coordination. The PEI/PSS/BiPE film shows the characteristic $\pi-\pi^*$ transition at 290 nm of the (uncoordinated) bipyridine groups. Different experimental protocols are explored for multilayer formation (see Figure 4).

In protocol A, alternating immersion of the substrate in solutions containing (a) $(NH_4)_2Fe(SO_4)_2$ and (b) BiPE, followed by rinsing, results in multilayer formation. Film growth is indicated by an increase of the MLCT bands and the $\pi-\pi^*$ transition (Figure 4). The appearance of the MLCT band and the shift of the $\pi-\pi^*$ transition proves metal ion coordination (vide supra) and formation of tris−bipyridine complexes during layer growth.

The insert in Figure 4 shows the absorbance at 540 nm as a function of the number of layers for different experimental protocols (A, B, C, D). Although layer growth in method A is not as regular as with PSS (vide supra), the increase of the absorbance follows a straight line, which confirms linear growth. In method B, the wafer is rinsed in water after each Fe(II) deposition. In this case, the layer thickness is smaller compared to that in protocol A; however, multilayer growth is still regular and linear. In method C, the wafer is rinsed in water after each BiPE and Fe(II) deposition. In these latter cases, layer growth is less efficient as indicated by the moderate slopes compared to method A. Finally, in the absence of metal ions (method D), there is no multilayer formation, which proves the importance of metal ion−ligand interactions for layer formation.

Figure 5 shows the RAIR spectra of 10 layers of BiPE deposited by metal ion coordination. The bands at 1596, 1557, 1486, and 1421 cm^{-1} are the characteristic ring breathing modes of pyridine. The peak at 1009 cm^{-1} is due to chelation of Fe(II) by bipyridine and is assigned to a pyridine breathing mode.[47] That the layer is hydrated is demonstrated by the occurrence of a broad

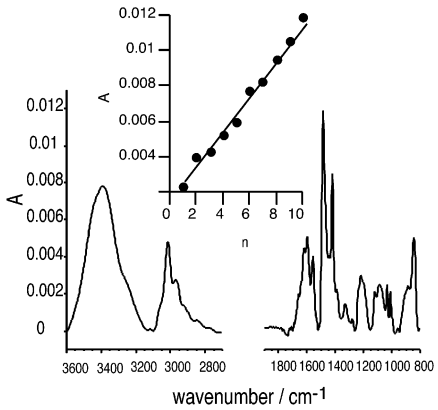

Figure 5. RAIR spectrum of a PEI/PSS(Fe(II)−BiPE)$_{10}$ multilayer. The insert shows the increase of the IR absorbance at 1486 cm^{-1} as a function of the number of layers, indicating linear layer growth.

band at 3400 cm^{-1}. The shoulder at 3200 cm^{-1} is attributed to the asymmetric stretch of the ammonium counterions. The presence of ammonium is also confirmed by the deformation mode at 1421 cm^{-1}. The sulfonate counterion is also present in the layers as indicated by the band at 1093 cm^{-1}. The band positions, widths, and relative intensities of the multilayer are comparable to those measured in the transmission spectrum of precipitated Fe(II)−BiPE. The similarity of the infrared spectra suggests that the structure of the precipitated bulk phase is similar to that of multilayers. Therefore, we propose that layer growth by metal ion coordination is primarily caused by formation of an insoluble cross-linked network. Possibly, there are two factors that contribute to cross-linking at the interface. (1) Vacant coordination sites at Fe(II) ions, such as in $Fe(bipy)^{2+}$ and $Fe(bipy)_2{}^{2+}$, may be present at the interface. Such complexes could arise due to the high excess of Fe(II) in deposition step (a). (2) It is known that 3-d transition metal ions, such as Fe(II), form kinetically labile complexes. We can, therefore, envision that (uncoordinated) bipy groups of BiPE from solution replace (coordinated) bipy groups of surface-confined $Fe(bipy)_3{}^{2+}$ complexes. Such ligand exchange reactions may, therefore, also contribute to film growth.

The resulting multilayers are rougher than the BiPE/PSS layers, as indicated by ellipsometry, AFM, and the absence of Kiessig fringes in XRR. After deposition of a PSS/PDADMAC layer pair the interface becomes smooth and Kiessig interference fringes become discernible in XRR. In the case of a PEI/PSS(Fe(II)−BiPE)3/PSS/PDADMAC multilayer, the total thickness is determined to be 106 Å. The thickness of a single BiPE layer is, therefore, estimated to be 15−17 Å, which is independently confirmed by optical ellipsometry.

The surface coverage is determined from the absorbance at 544 nm because e_λ is sufficiently small at this wavelength for reflection losses to be negligible. For the first layer the area per chromophore is approximately 5.2×10^{-7} mmol/cm^2 (32 Å^2), which stabilizes after three layers to a constant value of 3.2×10^{-7} mmol/cm^2 (53 Å^2). The area of an $Fe(bipy)_3{}^{2+}$ unit is estimated to be 140 Å^2, so the surface coverage is approximately 260%, which is in agreement with the previous result. We conclude that BiPE adsorbs in a coiled conformation.

(47) Sinha, S. P. *Spectrochim. Acta* **1964**, *20*, 879−886.

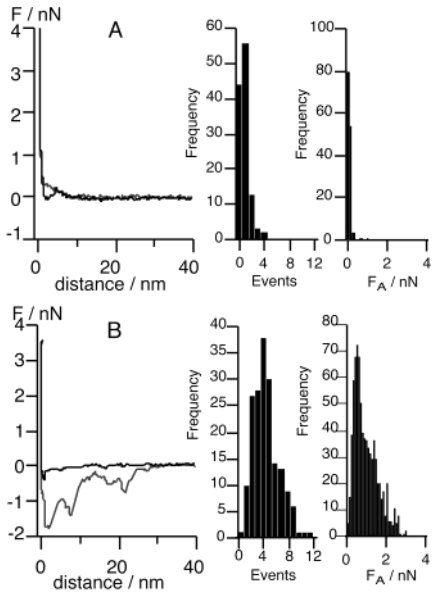

Figure 6. Representative force−distance curves before (A) and after (B) incubation of the sample in a 0.1 M $NiCl_2$ solution measured in 10 mM NaCl. The histograms show the distribution of the adhesion events and of the corresponding adhesion forces.

No signs of decomposition are observed if (Fe(II)−BiPE)$_n$ multilayers are immersed in water during the course of a week. The significance of the chelating metal ion receptor is demonstrated by performing additional control experiments using poly(vinyl-4-pyridine): no film growth was observed with this polymer under otherwise identical experimental conditions. However, immersing the Fe(II)−BiPE multilayer in a solution containing EDTA at pH = 10 at a temperature of 55 °C results in instant disassembly of the film. UV/vis spectroscopy reveals that all BiPE layers except the first one are removed. The first BiPE layer is not affected by EDTA because it adsorbs primarily through electrostatic interactions to the underlying PSS layer. We conclude that EDTA diffuses in the multilayer and coordinates the bound metal ions, which results in break up of the interlayer bonds and disassembly of the network. Experiments with $NiCl_2$ as an interlayer linker gave similar results in terms of multilayer growth, surface coverage, and stability.

Probing Metal Ion Coordination with Atomic Force Microscopy. The influence of metal ion coordination on the adhesion of adjacent BiPE layers is demonstrated by force−distance curves measured with AFM. The tip of the AFM cantilever is modified with a microscopic borosilicate particle to have a large and well-defined contact area. The surface of the particle is coated with a PEI/PSS/PAH/PSS/BiPE multilayer. Likewise, a silicon wafer is modified with an analogous PEI/PSS/PAH/PSS/BiPE multilayer. Both interfaces are terminated with BiPE to facilitate metal ion coordination upon contact of the particle-modified AFM tip and the surface. Force−distance curves are measured with the AFM in aqueous solution containing 10 mM NaCl.

A representative force−distance curve in the absence of transition metal ions is shown in Figure 6A. At large separation between the two surfaces there is no physical interaction and as a result no change in the cantilever position. During the approach of the tip we observe a long-range repulsive force between the equally charged interfaces, which is attributed to electrostatic interactions causing the cantilever to bend. Upon withdrawal after contact we observe few rupture events as the two surfaces separate. These events are attributed to unspecific steric and electrostatic interactions of possibly entangled polyelectrolytes under the influence of the applied force during the approach. To examine the influence of metal ion coordination, the same silicon wafer is immersed afterward in a solution containing 0.1 M $NiCl_2$ for 20 min. After rinsing the wafer with water, we record another series of force−distance curves. A typical example is shown in Figure 6B. At large separations the cantilever position does not change because there are no interactions. Then, we notice a short-range attractive interaction during the approach of the tip to the surface, which causes the cantilever to bend. Upon withdrawal of the tip we now observe a large number of rupture events, which are attributed to metal ion−ligand as well as electrostatic interactions between the two interfaces. We interpret this observation as follows. The metal ions yield a binding force between the two interfaces through metal ion coordination. If we assume that metal ion coordination is stronger than electrostatic interactions, withdrawal of the tip will first pull apart and stretch the cross-linked polyelectrolyte network between the two interfaces until eventually the metal ion−ligand bonds begin to rupture. As a result, the rupture events in the force−distance curves are generally broad, typical for elastically deformable connected networks. Therefore, we conclude that the attractive interactions revealed in the force−distance curves result from *multiple* interactions, including electrostatic interactions of entangled polyelectrolytes as well as metal ion coordination. With this procedure we, therefore, measure the overall interactions between the two interfaces. The overall procedure is repeated for a defined number of experiments and added together, yielding a histogram. A summary of the data on the rupture events and corresponding forces for a series of force−distance curves is shown in Figure 6 for repeated approach−withdrawal cycles at one spot on the surface. Clearly, the presence of $NiCl_2$ has a profound influence on the number and distribution of the rupture events and forces. In a first approximation, the force, F, necessary to break the metal ion−ligand interaction can be estimated if we assume that the energy, E_{ML}, of the metal ion−receptor interaction is independent of the distance, r. Assuming a metal ion−ligand distance of 2 Å, the resulting force is estimated by the equation $F = (E_{ML}/N_A)/r$ to be 1.1 nN.[48] In fact, Gaub et al. measured single metal ion coordination interactions in the range of 22−58 pN for the *N*-nitrilo-triacetic acid-hystidine system and different metal ions.[49] Clearly, the measured forces of up to 3 nN correspond to multiple interactions. However, at this point it is not possible to assess the number of interactions.

(48) Boland, T.; Ratner, B. D. *Proc. Natl. Acad. Sci. U.S.A.* **1995**, *92*, 5297−5301. For the estimate we used tabulated values for the enthalpy of the Fe(bipy)$_3$ complex (see Alexander, R. D.; Buisson, D. H.; Dudeney, W. L.; Irving, R. J. *J. Chem. Soc., Faraday Trans. 1* **1978**, *74*, 1081−1088.).

(49) Schmitt, L.; Ludwig, M.; Gaub, H. E.; Tampe, R. *Biophys. J.* **2000**, *78*, 3275−3285.

Various control experiments are performed to confirm these findings. For instance, if we measure force−distance curves of the two interfaces in a solution containing $NiCl_2$, the number of events and the adhesion forces are significantly lower. In this case, the metal ion receptors on both interfaces are already occupied by Ni ions, therefore reducing the probability of binding if the two surfaces approach each other. The replacement of the BiPE layer by a noncoordinating polyelectrolyte such as poly(diallyldimethylammonium chloride) (PDADMAC) on one or both interfaces under otherwise identical conditions leads to a distribution of rupture forces as in the absence of transition metal ions as shown in Figure 6A.

Conclusions

We present a versatile and modular approach for incorporating "value-adding" properties of metallo-units into thin films assembled by the ELSA method. A novel polyelectrolyte (BiPE) is employed that has permanent positive charges and metal ion receptors. High-quality multilayers are readily fabricated by alternate deposition of BiPE and an oppositely charged polyelectrolyte, such as PSS. Transition metal ions can be incorporated into the multilayers either by adsorption from solution or microcontact stamping. The latter approach results in spatially confined regions of metallo-units. Although not demonstrated here, there is little doubt that different metallo-units can be patterned in the layers, which may give rise to vectorial transport properties in the plane of the layers. Through a competing complexing agent, such as EDTA, the metal ions are removed from the film. Multilayer formation is also possible by metal ion coordination between layers by alternate deposition of transition metal ions and BiPE. Film growth is linear; however, the resulting interface is not as smooth as that of the ELSA multilayers. These metal ion coordinated layers readily disassemble upon exposure to EDTA, which opens interesting opportunities for controlled release applications. The quality of these metal ion coordinated multilayers could be improved in several ways, including the length of the polymer, the reversibility of metal ion coordination, and the assembly protocol. Strong binding between layers through metal ion coordination is confirmed by force−distance curves measured by AFM. Metal ion interactions are measured between the modified surfaces of a flat substrate and a colloidal particle attached to the AFM tip. The presence of metal ions has a profound influence on the number of rupture events and the interaction forces. Although it is not possible with this approach to investigate single interactions, it is possible to study the overall effect of strong interactions, such as metal ion coordination, because the receptors are firmly attached through multiple bonds to the underlying substrate. The number of metal ions participating in binding may be determined by a simultaneous electrochemical experiment.

The presented approach opens a straightforward route toward predefined deposition of transition metal ion complexes at interfaces, including planar surfaces and colloidal particles. The method is of general utility and applies to many transition metal ions, provides nanometer control of the film thickness, and is readily automated. Obviously, interfaces terminated with metal ion receptors can be linked through metal ion coordination, giving rise to novel composite materials, e.g., in the case of nanoparticles. In addition, new tools become available to investigate thin films, including absorption, fluorescence, electrochemistry, and AFM. These types of films may lead to a variety of technological applications, including metal ion sensors, such as ion-selective electrodes or membranes, as well as responsive layers, for example, for stimulus-triggered release. While our initial purpose was meant as a proof of principle, it became clear at the end of this study that metal ion coordination adds a rich flavor to multilayers in terms of fabrication, characterization, and function.

Acknowledgment. Financial support through the Deutsche Forschungsgemeinschaft is greatly appreciated. Helmuth Möhwald is acknowledged for valuable discussions and his support. The authors especially thank Christa Stolle for her contributions in synthesizing the compounds. Hauke Schollmeyer is acknowledged for performing the X-ray experiments.

CM020808D